

## Supporting Information

### **GalNAc-Functionalized Metal-Organic Frameworks for Targeted siRNA Delivery: Enhancing Survivin Silencing in Hepatocellular Carcinoma**

Xiuyan Wan,<sup>†,a</sup> Yingli Ge,<sup>†,a</sup> Wanqi Zhu,<sup>a</sup> Jie Zhang,<sup>a</sup> Wei Pan,<sup>a</sup> Na Li,<sup>\*,a</sup> and Bo Tang<sup>\*,a,b</sup>

[a] College of Chemistry, Chemical Engineering and Materials Science, Key Laboratory of Molecular and Nano Probes, Ministry of Education, Collaborative Innovation Center of Functionalized Probes for Chemical Imaging in Universities of Shandong, Institute of Molecular and Nano Science, Shandong Normal University, Jinan 250014, P. R. China.

[b] Laoshan Laboratory, Qingdao, 266237, P. R. China

[\*] lina@sdu.edu.cn (N. Li)

[\*] tangb@sdu.edu.cn (B. Tang)

[†] These authors contributed equally to this work.

## EXPERIMENTAL SECTION

### Materials and Instruments.

4,4,4,4-(Porphine-5,10,15,20-tetrayl)tetrakis (benzoic acid) was purchased from Shanghai Macklin Biochemical Technology Co., Ltd. N,N-Dimethylformamide (DMF) was purchased from Shanghai National Medicines Co., Ltd. Difluoroacetic acid, Zirconyl chloride octahydrate, (2S,3R,4R,5R,6R)-3-Acetamido-6-(Acetoxymethyl) Tetrahydro-2H-Pyran-2,4,5-Triyl Triacetate (GalNAc-5OAc), 2-Azidoethanol, trimethylsilyl trifluoromethanesulfonate (TMSOTf) and triethylamine (TEA) were purchased from Shanghai Adamas Reagent Co., Ltd. 3-(4,5-dimethyl-thiazole-2-yl)-2,5-diphenyltetrazolium bromide (MTT), was purchased from Beijing Solarbio Science & Technology Co., Ltd. Hoechst 33342, propidium iodide (PI), and calcein acetoxymethyl ester (Calcein-AM) were purchased from Beyotime Biotech. Inc. Anti-Caspase 3/CASP3 (p17) Antibody and FITC conjugated affinipure goat anti-rabbit IgG (H+L) were purchased from Boster Biological Technology Co., Ltd. Survivin siRNA (sense: 5'-AAGGAGAUCAACAUUUUCA-3'; antisense: 5'-UGAAA AUGUUGAUCUCCUU-3') and survivin siRNA<sup>cy5</sup> (Modification mode: 5'-cy5-3') were synthesized by Sangon Biotechnology Co. Ltd. (Shanghai, China). The Human hepatocellular liver carcinoma cell line (HepG2) was purchased from Wuhan Punosai Life Technology Co., Ltd. Balb/c-nu male mice (4-6 weeks, 18 - 20 g) were obtained from SiPeiFu Beijing Biotechnology Co., Ltd. Fetal bovine serum (FBS) in cell culture medium was purchased from Gibco. The experimental water used was Mill-Q secondary ultrapure water (18.2 M $\Omega$ ·cm<sup>-1</sup>). All the other chemical reagents were of analytical grade and used without further purification.

### Instruments.

Transmission electron microscopy (TEM, HT7700, Japan) was carried out to characterize the morphology of the nanoparticles. The Zeta potential was monitored with a Malvern Zeta Sizer Nano (Malvern Instruments). Fourier infrared spectrometer (Nicolet iS50 FT-IR) was used to characterize the FT-IR spectra. All pH measurements were performed with a pH-3c digital pH-meter (Shanghai LeiCi Device Works,

Shanghai, China) with a combined glass-calomel electrode. Absorbance in MTT assay was measured in a microplate reader (RT 6000, Rayto, USA). Confocal fluorescence imaging experiments were performed with TCS SP8/SP5 confocal laser scanning microscopy (Leica Co., Ltd. Germany) with a 20× objective. Live animal imaging system (IVIS Lumina III, US) was applied in vivo imaging. The MRI system was employed to detect the tumor volume of HepG2-bearing mice in the period of observation. Fluorescence spectra were obtained with FLS-980 Edinburgh. The concentration and UV-Vis absorbance of siRNA were performed on Nanodrop one (Thermo Scientific, USA). Native polyacrylamide gel electrophoresis analysis was performed on gel electrophoresis apparatus (Bio-Rad, USA). Peiqing JS-680D Automatic digital gel imaging analysis system was purchased from Peiqing Science & Technology Co., Ltd.

#### **Synthesis of MOF.**

The MOF with PCN-222 structure was created using a solvent-thermal synthesis method.  $ZrOCl_2 \cdot 8H_2O$  (37.7 mg, 0.117 mmol), TCPP (6.8 mg, 0.0086 mmol), and DFA (0.226 mL, 3.59 mmol, 416 equiv) were combined in DMF (16 mL) and heated at 120 °C for 24 h. The resulting mixture was then centrifuged, washed with DMF and acetone three times, and finally dried overnight.

#### **Synthesis of MOF-GalNAc.**

The MOF and GalNAc were mixed in a 1:0.7 mass ratio, and MOF-GalNAc was obtained by oscillating for 5 h. GalNAc was initially aminated. The aminated GalNAc was more easily modified on MOFs, increasing the synthesis efficiency of MOF-GalNAc by over 10%.

#### **Release of siRNA.**

To investigate the release of siRNA, siRNA@MOF-GalNAc nanoparticles were incubated in PBS (pH 7.4) for specific time intervals. The supernatant was collected at 0, 5, 10, 33, 48, 60, 69, 90, and 120 h and the siRNA concentration in the supernatant was measured using Nanodrop One.

#### **Cell Culture.**

HepG2 cells were cultured in MEM medium containing 10% fetal bovine serum, 1%

antibiotics (penicillin/streptomycin) and were maintained at 37 °C in a 5% CO<sub>2</sub>/95% air humidified incubator.

MCF-7, A549 cells were cultured in DMEM medium containing 10% fetal bovine serum, 1% antibiotics (penicillin/streptomycin) and were maintained at 37 °C in a 5% CO<sub>2</sub>/95% air humidified incubator.

#### **Flow cytometry.**

The material's targeting ability was assessed using flow cytometry. Three groups of cells were involved in the study: MCF-7, A549, and HepG2 cells. Each group of cells was treated with siRNA<sup>cy5</sup>@MOF-GalNAc (siRNA<sup>cy5</sup> concentration of 200 nM) and then incubated for 48 hours. Subsequently, the cells were collected, stained, and analyzed using flow cytometry.

#### **Live/Dead Cell Staining Assays.**

HepG2 cells were incubated in confocal dishes and divided into four groups: PBS, siRNA, siRNA@MOF, and siRNA@MOF-GalNAc. For each group, the HepG2 cells were treated with different nanoparticles (the final concentration of siRNA was 200 nM) for 48 h. After that, Calcein-AM and PI solutions were stained in PBS buffer for 20 min. Finally, the cells were washed three times with PBS and imaged using confocal laser scanning microscopy.

#### **Cell cloning experiment.**

7000 HepG2 cells were seeded in a 6-well plate and incubated with different nanoparticles. The cells were then incubated with the nanomaterials for 48 h, treated with paraformaldehyde for 15 min, stained with crystal violet for 20 min, and photographed afterward.

#### **In vivo experiments.**

Animal experiments were reviewed and approved by the Ethics Committee of Shandong Normal University, Jinan, P. R. China (approval number AEECSDNAU2023025). All the animal experiments complied with relevant guidelines of the Chinese government and regulations for the care and use of experimental animals.

#### **Establishment of orthotopic transplantation tumor model of liver cancer.**

Male Balb/c-nu mice aged 4-6 weeks and weighing about 18 - 20 g were kept in standard conditions with 12-hour light and dark cycles. They had unlimited access to food and water. HepG2 cells were treated with trypsin, washed with PBS three times, and then around  $1.4 \times 10^7$  of these cells were suspended in 75  $\mu$ L of serum-free MEM medium. This cell suspension was injected into the livers of the mice to create an orthotopic transplantation tumor model.

#### **In vivo fluorescence imaging.**

To investigate the targeting ability of MOF-GalNAc, ten days after establishing the mouse tumor model, IR808 and IR808@MOF-GalNAc (20 mg/kg) were intravenously administered into the tumor-bearing Balb/c-nu mice. At 0 h, 3 h, 6 h, 9 h, 12 h, 24 h, and 48 h after the injection of nanocarriers, the enrichment of nanocarriers in the mice tumor was detected using Bioluminescent Living Image. After 9 h, the heart, liver, spleen, lung, kidney, and tumor of the mice were dissected, and fluorescence imaging was performed.

#### **In vivo magnetic resonance imaging.**

Magnetic resonance imaging (MRI) was performed on the mice on the 10<sup>th</sup> day following the establishment of orthotopic tumors, as well as 7 and 14 days post-treatment.

#### **Statistics.**

Differences between pairs of mean values were evaluated for statistical significance using ANOVA, complemented by post-hoc Tukey-Kramer tests. Group comparisons were conducted via Student's t-test, with significance threshold set at P-values < 0.05 (\*p < 0.05, \*\*p < 0.01, \*\*\*p < 0.001). All statistical analyses were carried out employing Microsoft Excel software.

## SUPPORTING FIGURES

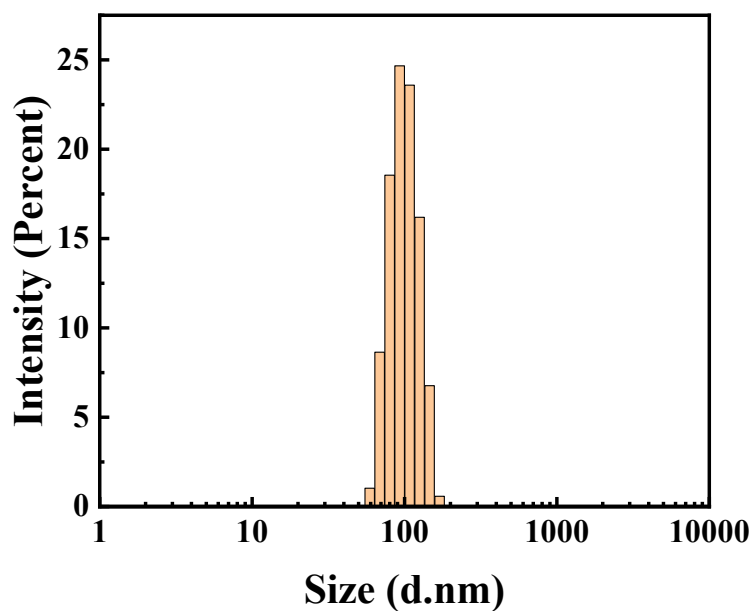


**Figure S1.** DLS measured size distribution of MOF, and the average size is  $91.54 \pm 1.49$  nm.

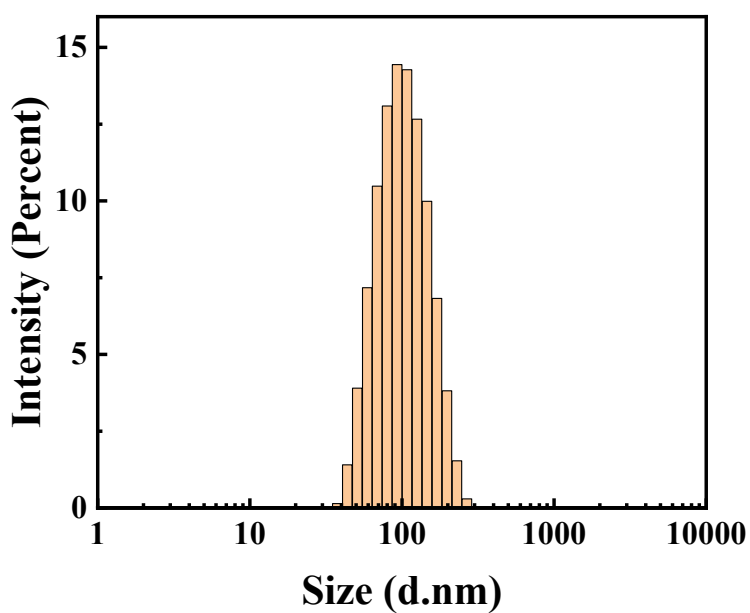


**Figure S2.** DLS measured size distribution of siRNA@MOF, and the average size is  $92.13 \pm 1.16$  nm.

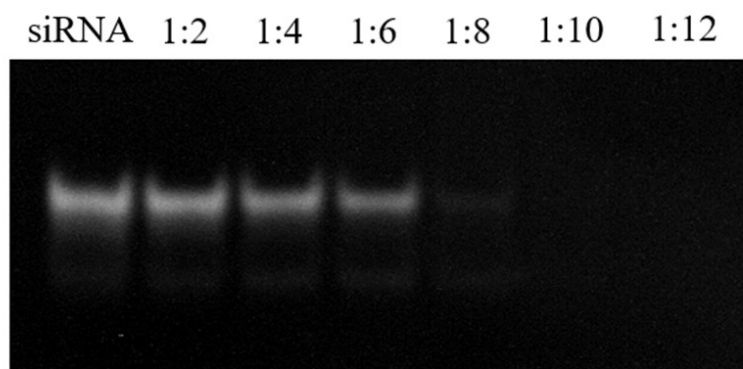


**Figure S3.** Polyacrylamide gel photograph of residue siRNA after loading into MOF with different ratio.

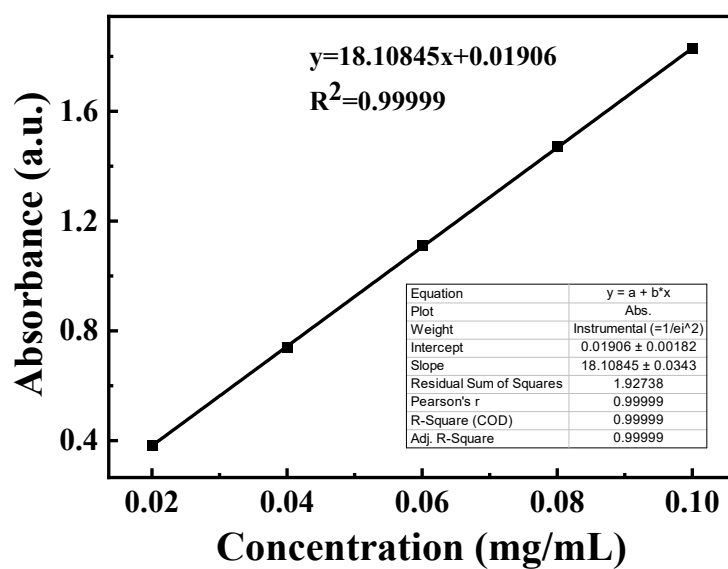


**Figure S4.** Linear relationships between the absorbance intensity of GalNAc and GalNAc concentration.

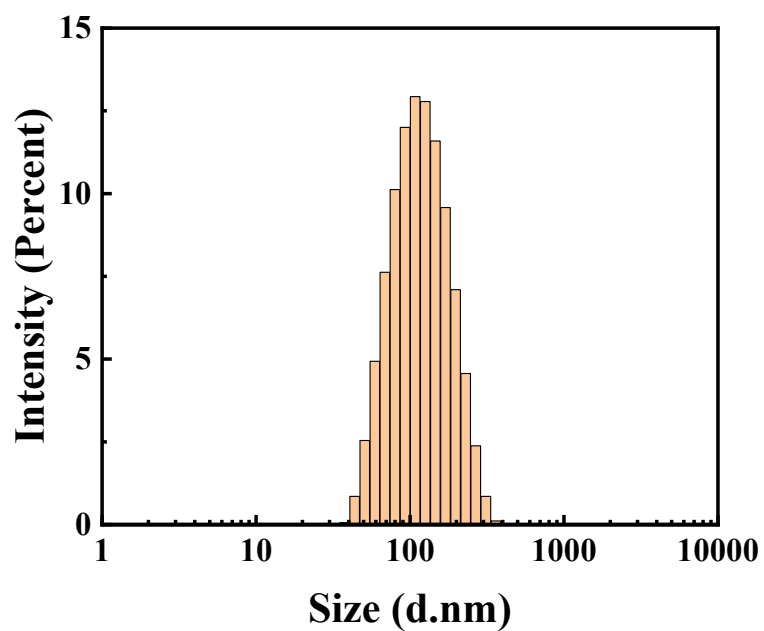


**Figure S5.** DLS measured size distribution of siRNA@MOF-GalNAc, and the average size is  $103.2 \pm 2.15$  nm.

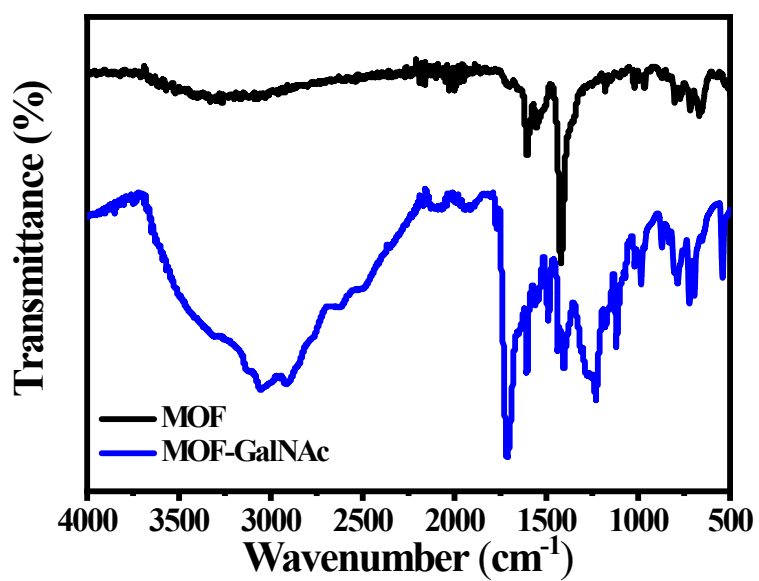


**Figure S6.** FTIR spectra of MOF (black) and MOF-GalNAc (blue).

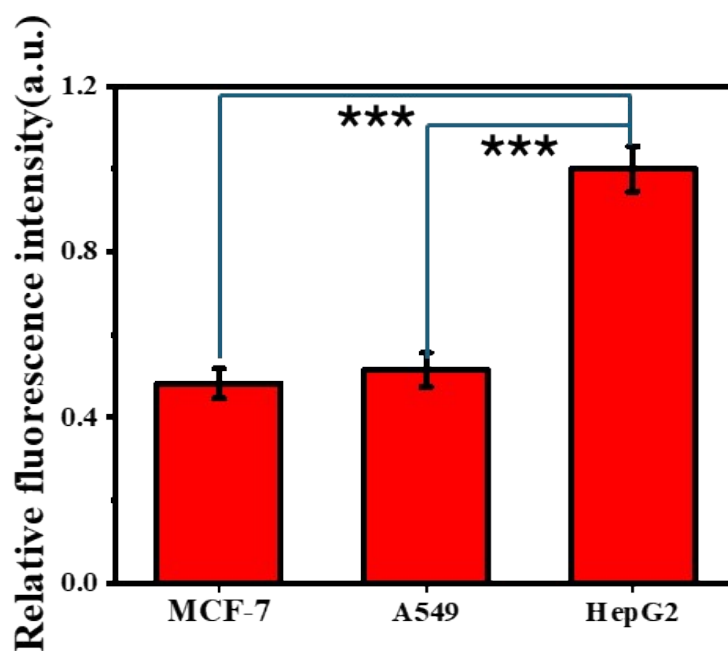


**Figure S7.** The relative fluorescence intensities of cy5 from siRNA<sup>cy5</sup>@MOF-GalNAc internalized by different cell lines in Figure 3a.

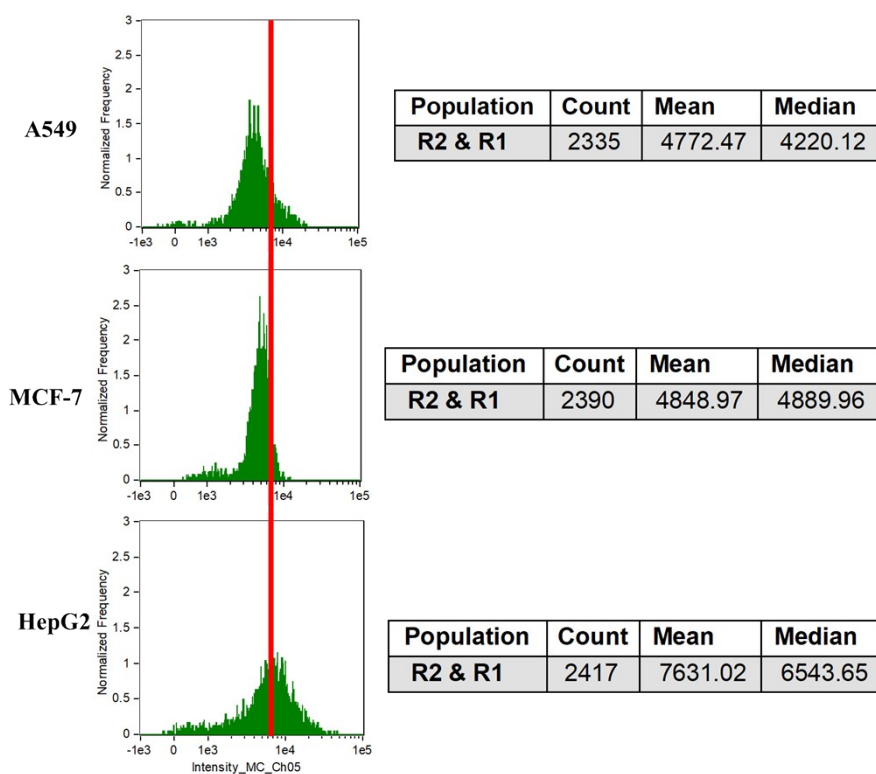


**Figure S8.** Flow cytometry analysis of the fluorescent intensity of cy5 from siRNA<sup>cy5</sup>@MOF-GalNAc internalized by different cell lines.

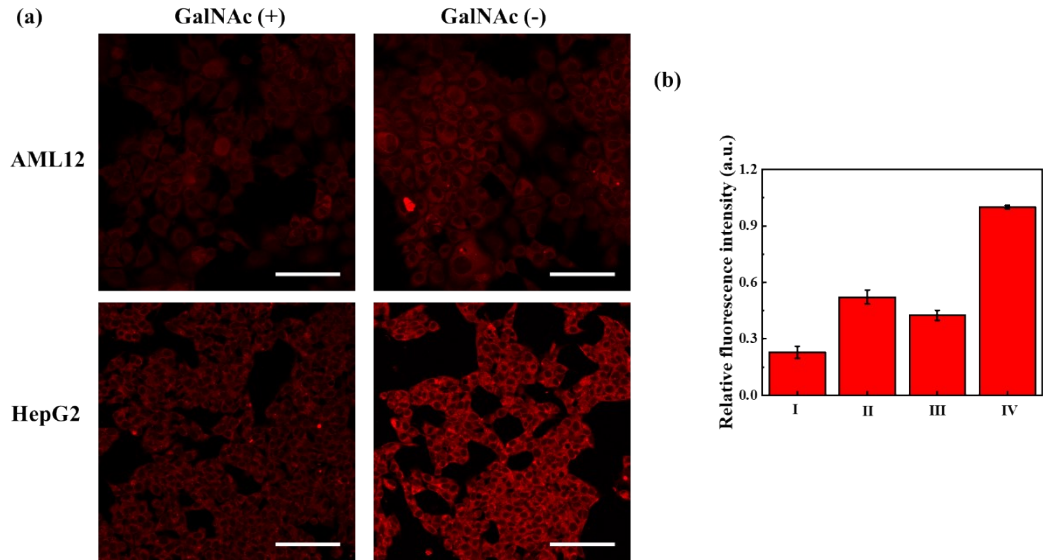


**Figure S9.** (a) CLSM images of AML12 and HepG2 cells treated with RhB@MOF-GalNac with (+) or without (-) pre-incubation of GalNac. Scale bars = 100  $\mu$ m. (b) The relative fluorescence intensities of RhB from RhB@MOF-GalNac internalized by different cell lines in Figure S9a (I: AML12 with GalNac; II: HepG2 with GalNac; III: AML12 without GalNac; IV: HepG2 without GalNac).

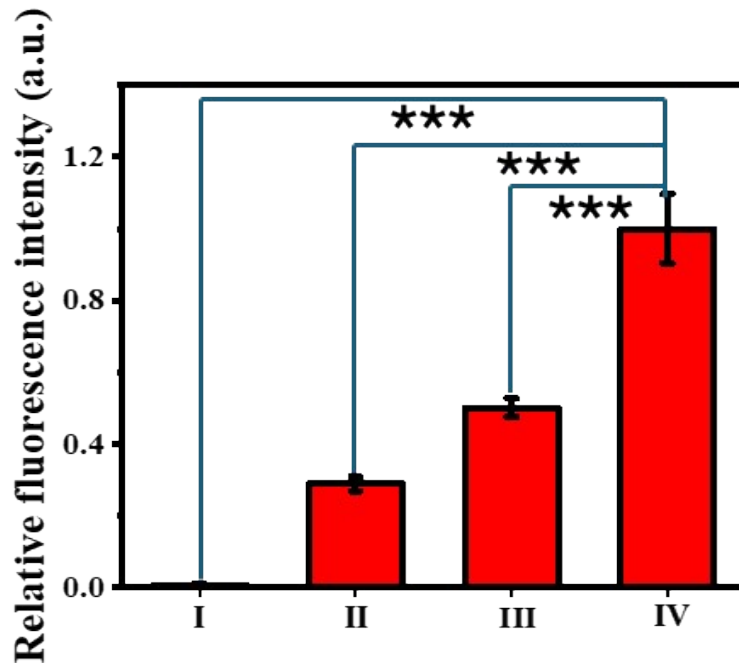


**Figure S10.** The relative fluorescence intensities of cy5 from PBS (I), siRNA<sup>cy5</sup> (II), siRNA<sup>cy5</sup>@MOF (III), and siRNA<sup>cy5</sup>@MOF-GalNac (IV) internalized by HepG2 cells in Figure 3b.

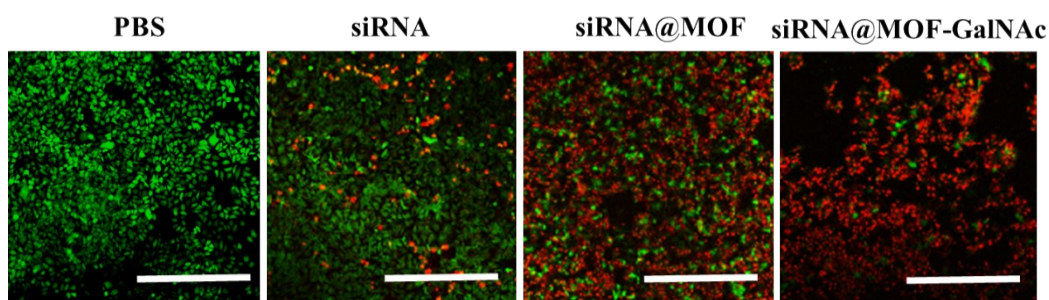


**Figure S11.** Live/dead cell staining assay of cells subjected to different treatments.

Scale bars = 250  $\mu\text{m}$ .

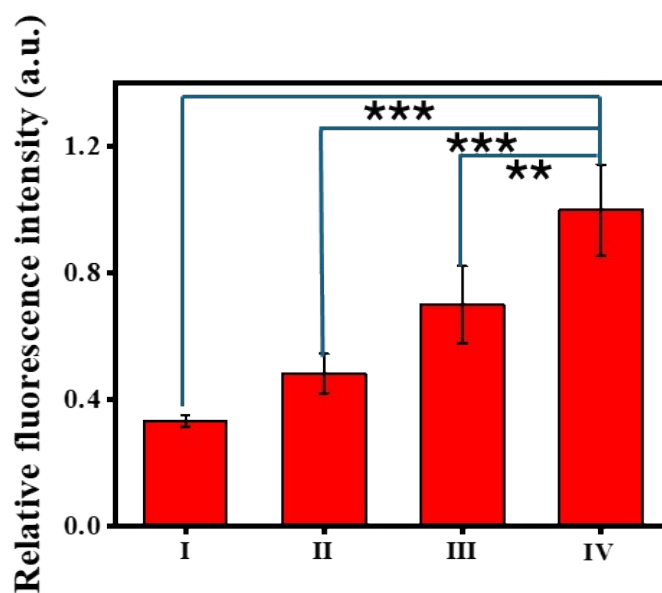


**Figure S12.** The relative fluorescence intensities in Figure 3f: PBS (I), siRNA (II), siRNA@MOF (III), and siRNA@MOF-GalNAc (IV).

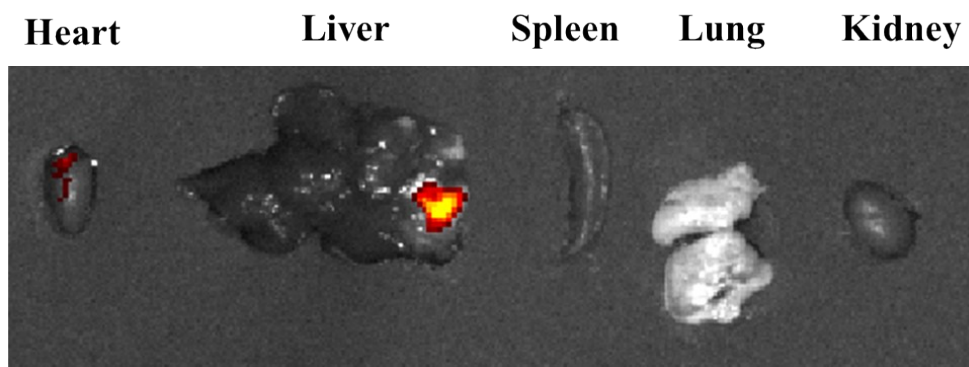


**Figure S13.** *Ex vivo* fluorescence images of major organs at 9 h post-injection of siRNA@MOF-GalNAc.

IR808@MOF-GalNAc.

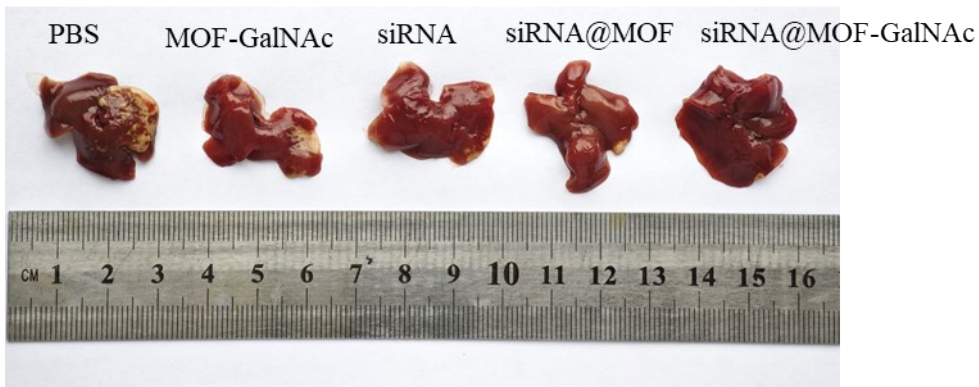


**Figure S14.** Representative photographs of liver from tumor-bearing mice in each group with different treatment.

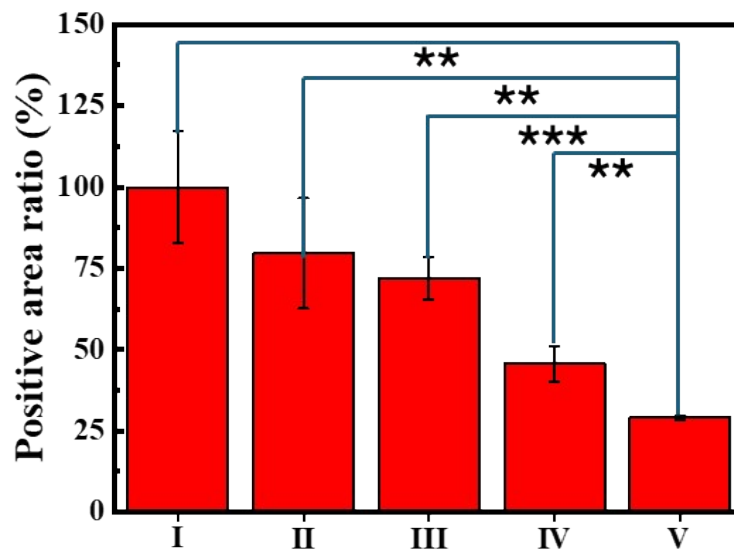


**Figure S15.** Quantification of Ki-67 immunohistochemical staining in tumor sections in Figure 4c (I: PBS; II: MOF-GalNAc; III: siRNA; IV: siRNA@MOF; V: siRNA@MOF-GalNAc).

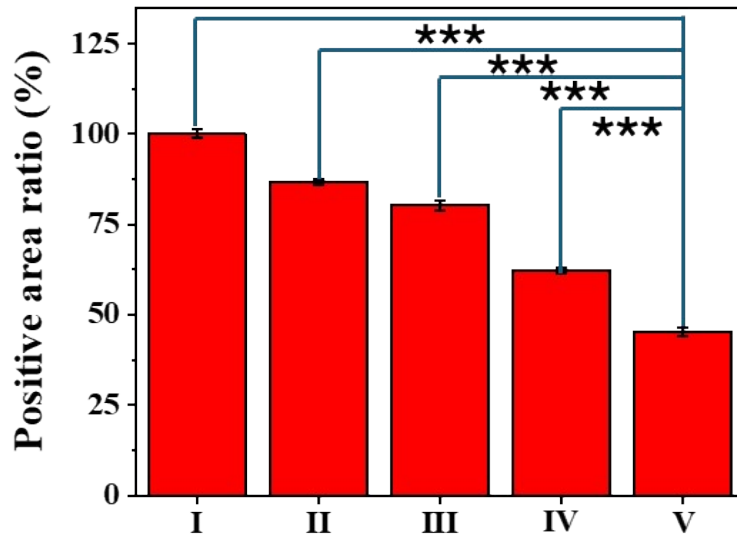


**Figure S16.** Quantification of survivin immunohistochemical staining in tumor sections in Figure 4d (I: PBS; II: MOF-GalNAc; III: siRNA; IV: siRNA@MOF; V: siRNA@MOF-GalNAc).

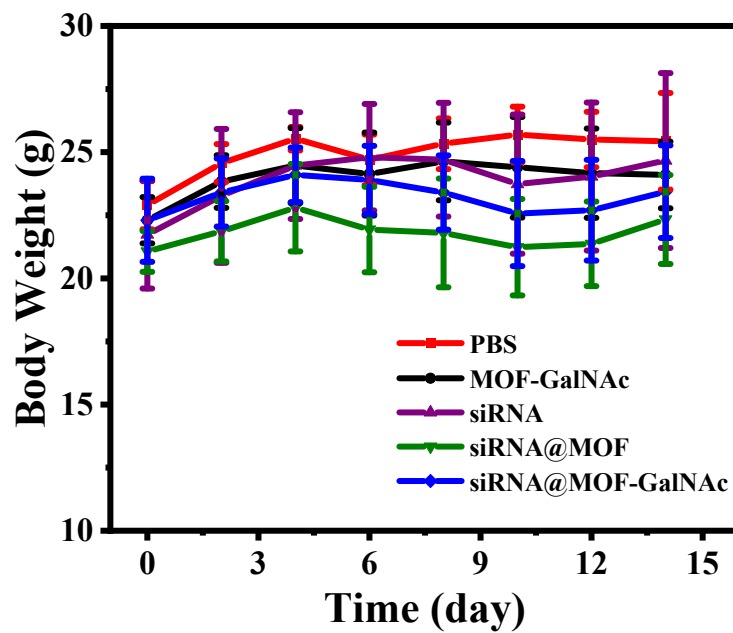


**Figure S17.** Body-weight changes of tumor-bearing mice within 14 days during treatment.

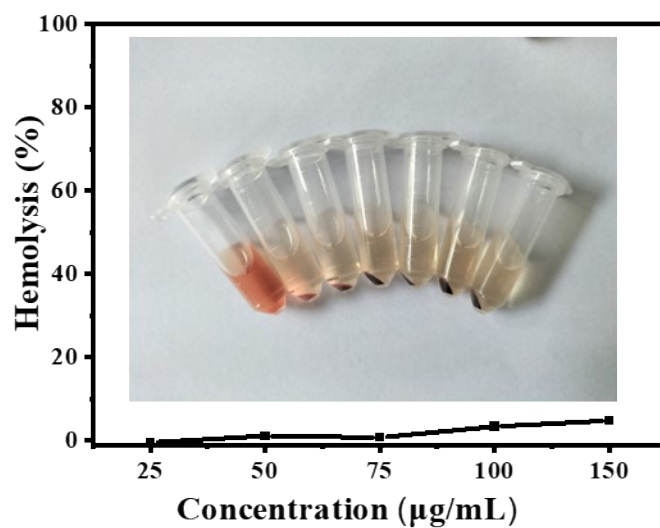


**Figure S18.** Analysis of hemolytic rates of different concentrations of siRNA@MOF-GalNac.

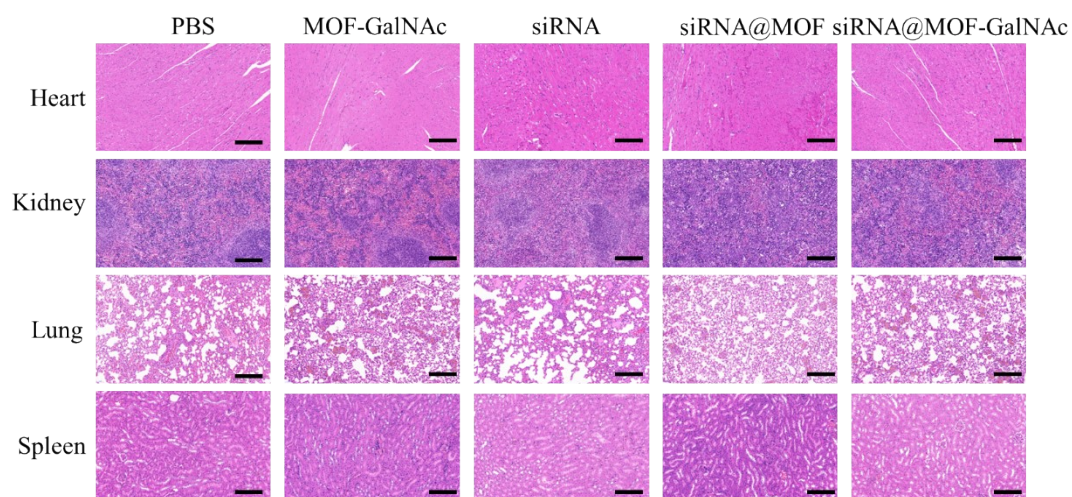


**Figure S19.** H&E staining of the four major organs with different treatments after 14 days. All scale bars are 200 µm.

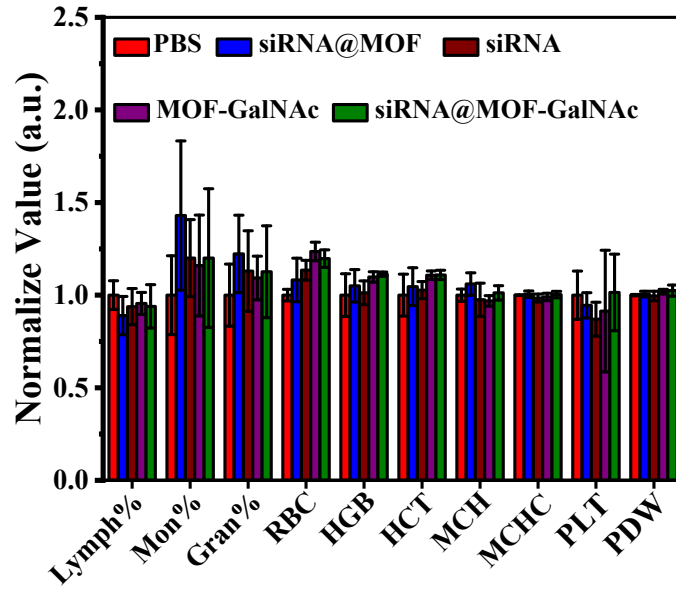
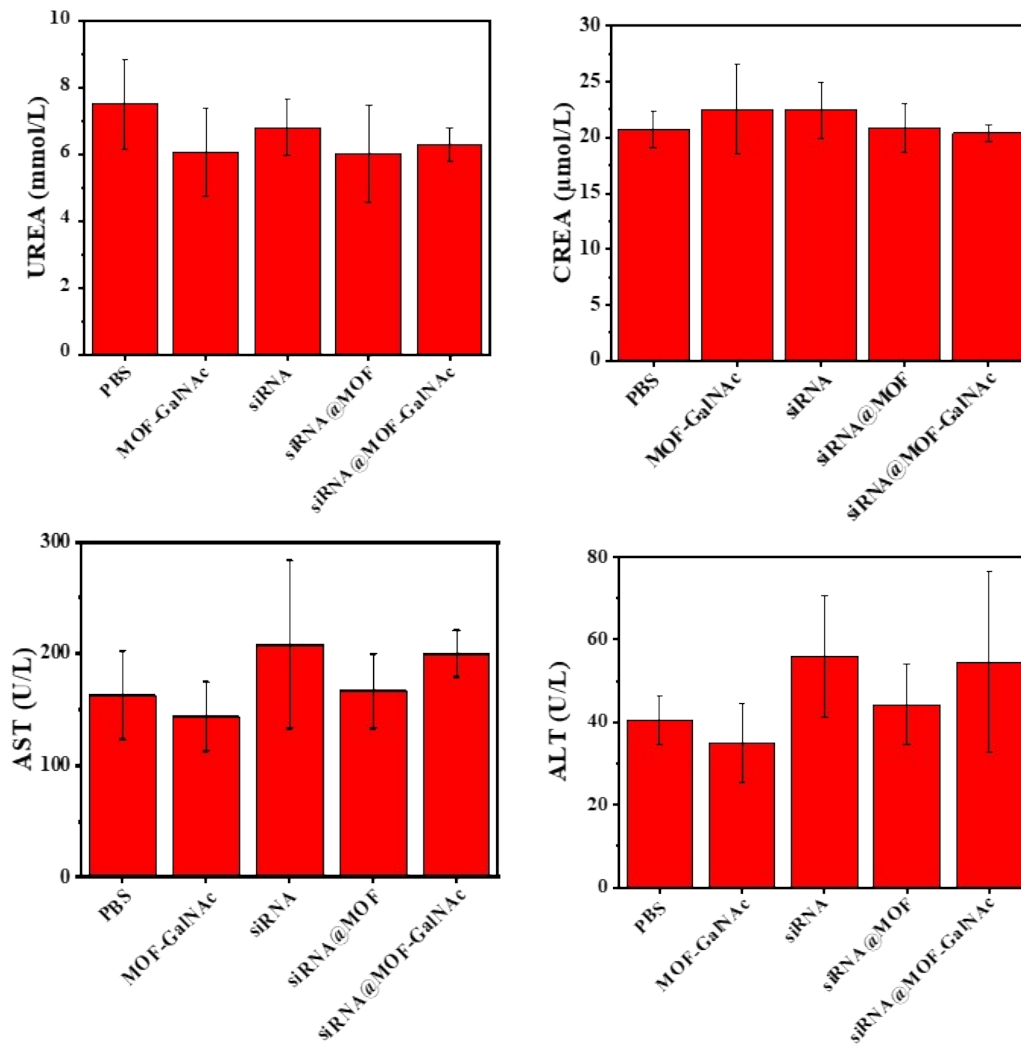


Figure S20. Hematological parameters of mice after different treatments.



**Figure S21.** Blood biochemical parameters of mice after different treatment